

Confinement of Activating Receptors at the Plasma Membrane Controls Natural Killer Cell Tolerance

Sophie Guia, Baptiste N. Jaeger, Stefan Piatek, Sébastien Mailfert, Tomasz Trombik, Aurore Fenis, Nicolas Chevrier, Thierry Walzer, Yann M. Kerdiles, Didier Marguet, Eric Vivier and Sophie Ugolini (5 April 2011)
Science Signaling 4 (167), ra21. [DOI: 10.1126/scisignal.2001608]

The following resources related to this article are available online at <http://stke.sciencemag.org>.
This information is current as of 3 October 2011.

- Article Tools** Visit the online version of this article to access the personalization and article tools:
<http://stke.sciencemag.org/cgi/content/full/sigtrans;4/167/ra21>
- Supplemental Materials** "Supplementary Materials"
<http://stke.sciencemag.org/cgi/content/full/sigtrans;4/167/ra21/DC1>
- Related Content** The editors suggest related resources on *Science's* sites:
<http://stke.sciencemag.org/cgi/content/abstract/sigtrans;4/175/ra36>
<http://stke.sciencemag.org/cgi/content/full/sci;332/6028/398-b>
<http://stke.sciencemag.org/cgi/content/abstract/sigtrans;4/167/pc7>
- References** This article has been **cited by** 2 article(s) hosted by HighWire Press; see:
<http://stke.sciencemag.org/cgi/content/full/sigtrans;4/167/ra21#BIBL>
- This article cites 54 articles, 18 of which can be accessed for free:
<http://stke.sciencemag.org/cgi/content/full/sigtrans;4/167/ra21#otherarticles>
- Glossary** Look up definitions for abbreviations and terms found in this article:
<http://stke.sciencemag.org/glossary/>
- Permissions** Obtain information about reproducing this article:
<http://www.sciencemag.org/about/permissions.dtl>

Confinement of Activating Receptors at the Plasma Membrane Controls Natural Killer Cell Tolerance

Sophie Guia,^{1,2,3*} Baptiste N. Jaeger,^{1,2,3*} Stefan Piatek,^{1,2,3} Sébastien Mailfert,^{1,2,3} Tomasz Trombik,^{1,2,3} Aurore Fenis,^{1,2,3} Nicolas Chevrier,^{1,2,3†} Thierry Walzer,^{1,2,3‡} Yann M. Kerdiles,^{1,2,3} Didier Marguet,^{1,2,3} Eric Vivier,^{1,2,3,4§} Sophie Ugolini^{1,2,3§}

Natural killer (NK) cell tolerance to self is partly ensured by major histocompatibility complex (MHC) class I–specific inhibitory receptors on NK cells, which dampen their reactivity when engaged. However, NK cells that do not detect self MHC class I are not autoreactive. We used dynamic fluorescence correlation spectroscopy to show that MHC class I–independent NK cell tolerance in mice was associated with the presence of hyporesponsive NK cells in which both activating and inhibitory receptors were confined in an actin meshwork at the plasma membrane. In contrast, the recognition of self MHC class I by inhibitory receptors “educated” NK cells to become fully reactive, and activating NK cell receptors became dynamically compartmentalized in membrane nanodomains. We propose that the confinement of activating receptors at the plasma membrane is pivotal to ensuring the self-tolerance of NK cells.

INTRODUCTION

How tolerance to self is ensured while mounting a protective response is a central issue for the organization of the immune system. Most of our present understanding of immune tolerance is based on the dissection of the mechanisms at work in T and B cells (1); however, the molecular pathways that ensure tolerance in innate immunity are still poorly understood. Natural killer (NK) cells are effector and regulatory lymphocytes of the innate immune system that contribute to tumor surveillance, hematopoietic allograft rejection, control of microbial infections, and pregnancy (2, 3). NK cells can be cytotoxic and secrete an array of cytokines and chemokines, such as interferon- γ (IFN- γ) and β -chemokines. Hence, the effector functions of NK cells must be tightly controlled to avoid immunopathology. The activation of NK cells is regulated by a large number of cell surface receptors, including activating receptors, inhibitory receptors, and adhesion molecules (4). Upon interaction with neighboring cells, the integration of these pathways governs the effector functions of NK cells (5, 6).

Self-tolerance of NK cells involves the dampening of their effector function through the recognition of self molecules constitutively expressed on interacting healthy cells by inhibitory receptors on the surface of NK cells. A prototypical example of this mode of recognition resides in the detection of self major histocompatibility complex (MHC) class I molecules through inhibitory killer cell immunoglobulin-like receptors (KIRs) in humans and their functional inhibitory Ly49 homologs in the mouse (4, 7, 8). In addition to sensing some microbial molecules, NK cells sense an array of self molecules, which are low in abundance or absent under normal conditions, but are increased in abundance under stressful con-

ditions, such as microbial infections, tumor transformation, and the physical or chemical insults that can activate the DNA damage response (9). Thus, NK cells spare healthy cells that have self MHC class I molecules and low amounts of stress-induced self molecules, whereas NK cells selectively kill target cells “in distress,” which have lower amounts of MHC class I molecules (“missing self”) and higher amounts of stress-induced self molecules, such as NKG2D (NK group 2-D) ligands, at the cell surface (9).

NK cells undergo maturation to acquire full competence as effector cells. The detection of self MHC class I through MHC class I–specific inhibitory receptors has a dual role: It controls the reactivity of NK cells at the immunological synapses (contact points) formed between NK cells and the cells with which they interact, and it is also involved in the education of NK cells to recognize cells with low amounts of MHC class I at the surface. This process of education was also referred to as “licensing,” “arming/disarming,” or “tuning” by some investigators (10–15). In humans and mice, several *KIR* and *Ly49* genes encode inhibitory receptors that recognize specific groups of MHC class I allele products (16). *KIR* and *Ly49* genes are polymorphic, inherited through the germline, and segregate independently of their MHC class I ligands. These genetic features and the variegated expression of *KIR* and *Ly49* molecules lead to the generation of a fraction of NK cells that do not have inhibitory receptors for self MHC class I molecules in humans and mice (10, 12). Thus, all NK cells are not kept in check by self MHC class I molecules, a condition that is exacerbated in MHC class I–deficient patients and mice (14, 15). In T and B cells, negative selection ensures the active death of autoreactive cells (1). In contrast, NK cells lacking inhibitory receptors specific for self MHC class I molecules, which could be potentially autoreactive, are tolerant to self because they are rendered hyporesponsive to stimulation through multiple activating receptors that are involved in the detection of target cells, such as NKp46, NKG2D, or mouse NK1.1 (14).

Mouse *Ly49* and human *KIR* MHC class I–specific inhibitory receptors mediate their inhibitory function through cytoplasmic immunoreceptor tyrosine-based inhibition motifs (ITIMs) that, in response to tyrosine phosphorylation, recruit the protein tyrosine phosphatases Src homology 2 (SH2) domain–containing protein tyrosine phosphatase 1 (SHP-1), SHP-2, or both (5, 6). Through SHP-1, the engagement of *KIR* stimulates the dephosphorylation of the guanine nucleotide exchange factor Vav1, which

¹Centre d’Immunologie de Marseille-Luminy, Université de la Méditerranée, Campus de Luminy case 906, 13288 Marseille, France. ²INSERM U631, 13288 Marseille, France. ³CNRS, UMR6102, 13288 Marseille, France. ⁴Assistance Publique–Hôpitaux de Marseille, Hôpital de la Conception, 13385 Marseille, France.

*These authors contributed equally to this work.

†Present address: Graduate Program in Immunology, Division of Medical Sciences, Harvard Medical School, Boston, MA 02115, USA.

‡Present address: Université de Lyon, INSERM U851, 21 avenue Tony Garnier, Lyon F-69007, France.

§To whom correspondence should be addressed. E-mail: ugolini@ciml.univ-mrs.fr (S.U.); vivier@ciml.univ-mrs.fr (E.V.)

leads to the inactivation of Rac1 (17). The KIR signaling pathway also induces the phosphorylation of the adaptor Crk, which leads to a block in actin-dependent processes, such as reorganization of the actin cytoskeleton or accumulation of lipid rafts at the immunological synapse (18).

Despite this knowledge, the MHC class I-independent mechanisms that control the hyporesponsiveness of NK cells and, conversely, the mechanisms at work in the MHC class I-dependent education of NK cells are still obscure (19). Here, we addressed these issues with several complementary mouse models to compare NK cells that did not undergo MHC class I-dependent education (which are referred to as hyporesponsive NK cells) and NK cells that were educated through the detection of self MHC class I through inhibitory receptors (which are referred to as competent NK cells). NK cells from MHC class I-deficient mice (K^bD^bKO mice) were the source of hyporesponsive NK cells. These cells were compared to those from wild-type C57BL/6 mice, in which most NK cells (around 85%) are competent (12). We also took advantage of a humanized transgenic mouse model that we recently described, in which all of the NK cells are rendered competent through the engagement of a single human inhibitory KIR by its cognate ligand HLA-Cw3 (K^bD^bKO -TgKIR/HLA mice) (20). The use of these transgenic mice revealed that NK cells could be reprogrammed to recognize the absence of self TgHLA and to control the development of mouse syngeneic tumors in vivo (20). This transgenic model also represents a powerful tool to overcome the complexity of the NK cell population in wild-type mice. Indeed, mouse inhibitory receptors are not uniformly expressed on NK cells, and inhibitory Ly49 receptors have various affinities for their H-2 ligands, which leads to a heterogeneous population of NK cells that are not rendered equally competent by education with self MHC class I molecules (11). In contrast, in the K^bD^bKO -TgKIR/HLA model, mouse MHC class I molecules are absent, but all of the cells have the human MHC class I molecule HLA-Cw3. In addition, all of the NK cells uniformly express KIR2DL3. The entire NK cell population can thus be educated through the interaction between KIR2DL3 and its ligand HLA-Cw3. We combined the use of these mouse models and the nanoscopic analysis of the mobility of surface receptors below the optical diffraction limit to show that the engagement of inhibitory receptors regulated the ultrafine, cell-membrane organization of activating receptors, providing a key mechanism for MHC class I-dependent NK cell education and MHC class I-independent NK cell tolerance.

RESULTS

NK cell education affects proximal signaling

To assess NK cell responsiveness, we stimulated NK cells freshly isolated from wild-type, K^bD^bKO , K^bD^bKO -TgKIR/HLA, and K^bD^bKO -TgKIR mice in vitro with monoclonal antibody (mAb) against NK1.1 (NK1.1 mAb). We chose NK1.1 (*Klrk1*) because it is an activating receptor that was uniformly expressed on all NK cells from our mice (Fig. 1A), and this experimental design enabled us to assess the intrinsic responsiveness of NK cells without interference from ligands potentially expressed on target cells. We stimulated cells for 4 hours with plate-bound NK1.1 mAb and measured single-cell production of IFN- γ by multiparametric flow cytometry. At the population level, NK cells from K^bD^bKO and K^bD^bKO -TgKIR mice were less responsive to stimulation of NK1.1 relative to NK cells from wild-type and K^bD^bKO -TgKIR/HLA mice, respectively (Fig. 1B). In addition to this reduction in the percentage of IFN- γ^+ NK cells, NK cells from K^bD^bKO and K^bD^bKO -TgKIR mice were also less responsive to NK1.1 stimulation as exhibited by the decrease in IFN- γ mean fluorescence intensity (MFI) among IFN- γ^+ cells in K^bD^bKO and K^bD^bKO -TgKIR cells relative to wild-type and K^bD^bKO -TgKIR/HLA NK cells, respectively (Fig. 1B). Data obtained from experiments with K^bD^bKO -TgKIR/HLA mice were comparable to

that obtained from experiments with K^bD^bKO -TgKIR mice, ruling out the contribution of any potential HLA-Cw3-dependent, but KIR-independent, mechanisms in the reactivity of NK cells from K^bD^bKO -TgKIR/HLA mice.

The cell surface abundance of KLRG1 (killer cell lectin-like receptor subfamily G member 1), a cadherin-specific inhibitory receptor, is decreased in the population of NK cells raised in an MHC class I-deficient background compared to that in wild-type NK cells (21). Although experiments with KLRG1-deficient mice revealed that this receptor is not required for the regulation of NK cell function (22), we used KLRG1 as a marker and observed that the percentage of KLRG1⁺ NK cells was also decreased in hyporesponsive NK cells from K^bD^bKO -TgKIR mice relative to that of NK cells from K^bD^bKO -TgKIR/HLA mice (Fig. 1B). Together with our earlier in vitro and in vivo data (20), these results suggest that NK cells from K^bD^bKO -TgKIR/HLA mice behaved similarly to those from wild-type mice, reinforcing the relevance of the side-by-side comparison between NK cells raised in wild-type and NK cells raised in K^bD^bKO mice and between NK cells from K^bD^bKO -TgKIR/HLA and NK cells from K^bD^bKO -TgKIR mice.

To determine whether NK cell hyporesponsiveness affected the early phases of NK cell activation, we examined calcium (Ca^{2+}) flux in response to NK1.1 mAb in NK cells from wild-type, K^bD^bKO , K^bD^bKO -TgKIR/HLA, and K^bD^bKO -TgKIR mice. The NK1.1-induced Ca^{2+} response was blunted in K^bD^bKO NK cells relative to that of wild-type NK cells (Fig. 1C). This impaired Ca^{2+} response was also observed in K^bD^bKO -TgKIR NK cells when compared to K^bD^bKO -TgKIR/HLA NK cells (Fig. 1C). We obtained similar results in experiments in which we stimulated NKG2D (Fig. S1). As a control, ionomycin, which bypasses cell surface receptors, led to strong and equivalent Ca^{2+} responses in NK cells from all of the mouse strains (Fig. 1C). Thus, the mechanisms involved in establishing MHC class I-independent NK cell tolerance had an effect on the proximal signaling pathways that are engaged downstream of various activating cell surface receptors.

Effect of education on the NK cell transcriptional program

We next performed pan-genomic microarray analysis to compare the transcriptional profiles of sorted populations of hyporesponsive and competent NK cells. To increase the likelihood of identifying genes involved in the effect of host MHC class I on NK cell reactivity, we compared wild-type NK cells to NK cells isolated from two different MHC class I-deficient mice, K^bD^bKO and $\beta 2mKO$ (tables S2 and S3). We conducted a similar analysis of NK cells isolated from K^bD^bKO -TgKIR/HLA and K^bD^bKO -TgKIR mice (table S1). To avoid potential confounding effects induced by the transgenic and knockout models themselves, we focused on the genes present in all three gene lists. A single gene, *Klra6*, was differentially expressed (by a factor of at least 1.7) between hyporesponsive NK cells (that is, K^bD^bKO , $\beta 2mKO$, and K^bD^bKO -TgKIR cells) and responsive NK cells (that is, wild-type and K^bD^bKO -TgKIR/HLA cells) (Fig. 2A). *Klra6* encodes the inhibitory Ly49F receptor, and *Klra6* mRNA was increased in abundance in hyporesponsive NK cells relative to responsive NK cells. This transcriptional modification was confirmed by reverse transcription-quantitative polymerase chain reaction (RT-qPCR) analysis, which revealed a factor of 1.7 increase in *Klra6* mRNA abundance in K^bD^bKO NK cells relative to wild-type cells, a factor of 1.5 increase in $\beta 2mKO$ NK cells relative to wild-type cells, and a factor of 3.5 increase in K^bD^bKO -TgKIR NK cells relative to K^bD^bKO -TgKIR/HLA NK cells.

NK cell education skews the Ly49 repertoire

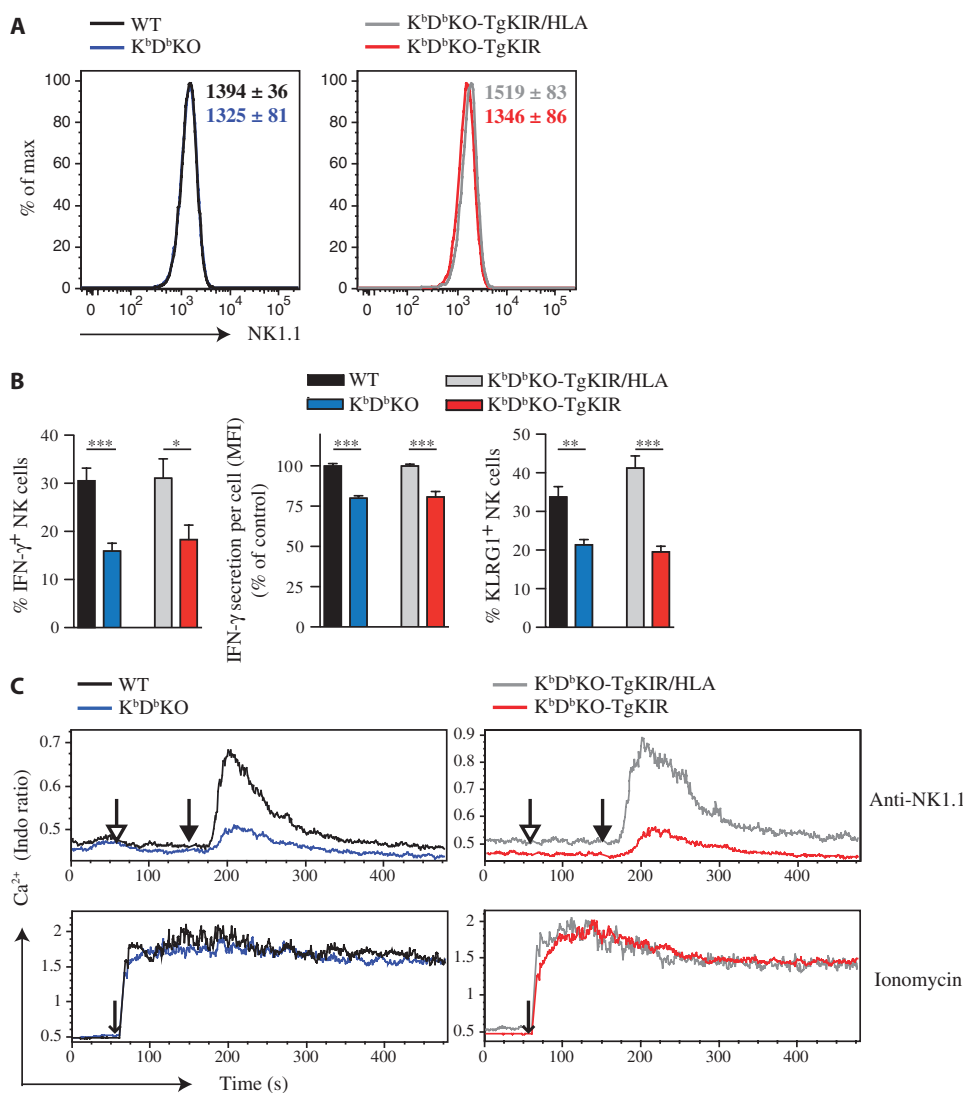
Ly49F is an inhibitory receptor encoded in the mouse NK gene locus, which includes genes encoding Ly49A, Ly49C, Ly49D, Ly49G2, Ly49H, and Ly49I in C57BL/6 mice (23). Of these, only Ly49C and Ly49I strongly re-

cognize the MHC class I molecule H2-K^b (23, 24), whereas Ly49A is thought to weakly interact with H-2D^b molecules (25). Ly49F may weakly recognize class I molecules encoded in the H-2^d MHC haplotype, but no ligands have been reported in the C57BL/6 background (24). Consistent with the transcriptional data, we found that the frequency of Ly49F⁺ NK cells was increased in the hyporesponsive NK cell population relative to the competent NK cell population, that is, when comparing wild-type NK cells with K^bD^bKO NK cells or K^bD^bKO-TgKIR/HLA NK cells with K^bD^bKO-TgKIR NK cells (Fig. 2B and fig. S2). Given the homology between all of the Ly49 receptors, it was possible that the probe sets used in the microarray analysis could not accurately distinguish between the receptors to detect variations in their abundance. Thus, we directly investigated at the protein level whether the cell surface expression of other Ly49 receptors was different between the hyporesponsive and the competent NK cell popula-

tions. Ly49A, Ly49C/I, and Ly49G2 were also overrepresented in the hyporesponsive NK cell population present in K^bD^bKO-TgKIR mice relative to the competent NK cell population present in K^bD^bKO-TgKIR/HLA mice (Fig. 2C and fig. S2). We observed a similar trend when we compared the hyporesponsive NK cell population from K^bD^bKO mice with the competent NK cell population from wild-type mice (Fig. 2C and fig. S2). The lower extent of the effect observed between wild-type and K^bD^bKO mice relative to that between K^bD^bKO-TgKIR and K^bD^bKO-TgKIR/HLA mice was likely a consequence of confounding effects because of the interaction between Ly49 and H-2^b molecules, a situation that is avoided in K^bD^bKO-TgKIR and K^bD^bKO-TgKIR/HLA mice.

Because the mouse NK gene locus also contains genes that encode activating receptors, we investigated whether the increased abundance of Ly49 that we observed in the population of hyporesponsive NK cells was specific

Fig. 1. The education of NK cells affects proximal signaling. (A to C) Flow cytometric analysis of (A) NK1.1 expression, (B) IFN- γ production, and (C) intracellular Ca²⁺ flux of fresh splenic NK cells isolated from wild-type (WT), K^bD^bKO, K^bD^bKO-TgKIR/HLA, and K^bD^bKO-TgKIR mice. (A) NK1.1 expression on NK cells that were defined as the NKp46⁺CD3⁻CD19⁻aqueadead⁻ population. Data are representative of two independent experiments (total of three mice per group). Numbers correspond to the geometric MFI \pm SEM. (B) Left and middle panels: Splenocytes were stimulated for 4 hours in vitro on plates coated with NK1.1 mAb. Intracellular IFN- γ production was measured in NKp46⁺CD3⁻aqueadead⁻ cells. Data show the frequencies of IFN- γ ⁺ NK cells among the total NK cell population (left panel) or the amount of IFN- γ secretion (MFI) per IFN- γ ⁺ NK cell (middle panel). MFI control values were calculated as the average of the IFN- γ MFI of IFN- γ ⁺ NK cells from WT or K^bD^bKO-TgKIR/HLA mice. For each experiment, these control values were compared to the IFN- γ MFIs of IFN- γ ⁺ NK cells isolated from K^bD^bKO and K^bD^bKO-TgKIR mice, respectively, to calculate the percentage compared to the control. Data were pooled from five to seven experiments with a total of 7 to 13 mice per group. Results are presented as the means \pm SEM. Statistical analysis was performed with the Mann-Whitney test. **P* < 0.05; ***P* < 0.01; ****P* < 0.001. (C) Ca²⁺ flux changes in freshly isolated NK cells were measured by flow cytometry. Top panels: After 1 min of acquisition, biotinylated NK1.1 mAb (anti-NK1.1) was added to the cells (open-headed arrow), followed 1.5 min later by streptavidin (closed-headed arrow) to induce NK1.1 cross-linking. Bottom panels: Maximal cell responsiveness was assessed by the addition of ionomycin (arrow). NK cells were defined as CD49b⁺CD3⁻ cells. Changes in intracellular Ca²⁺ over time are presented as the ratio of Indo-1 (violet) to Indo-1 (blue). Median



values of kinetics are shown. Data are representative of six experiments for WT and K^bD^bKO mice and two experiments for K^bD^bKO-TgKIR/HLA and K^bD^bKO-TgKIR mice. Each stimulation was repeated two to three times per experiment.

to inhibitory receptors. The abundance of the activating receptor Ly49H was not modulated in the wild-type versus K^bD^b KO NK cells, nor did it differ between K^bD^b KO-TgKIR/HLA and K^bD^b KO-TgKIR NK cells (Fig. 2D and fig. S2). We observed a slight decrease in the percentage of Ly49D⁺ NK cells when comparing wild-type and K^bD^b KO NK cells, but this was not confirmed in our second model (Fig. 2D and fig. S2).

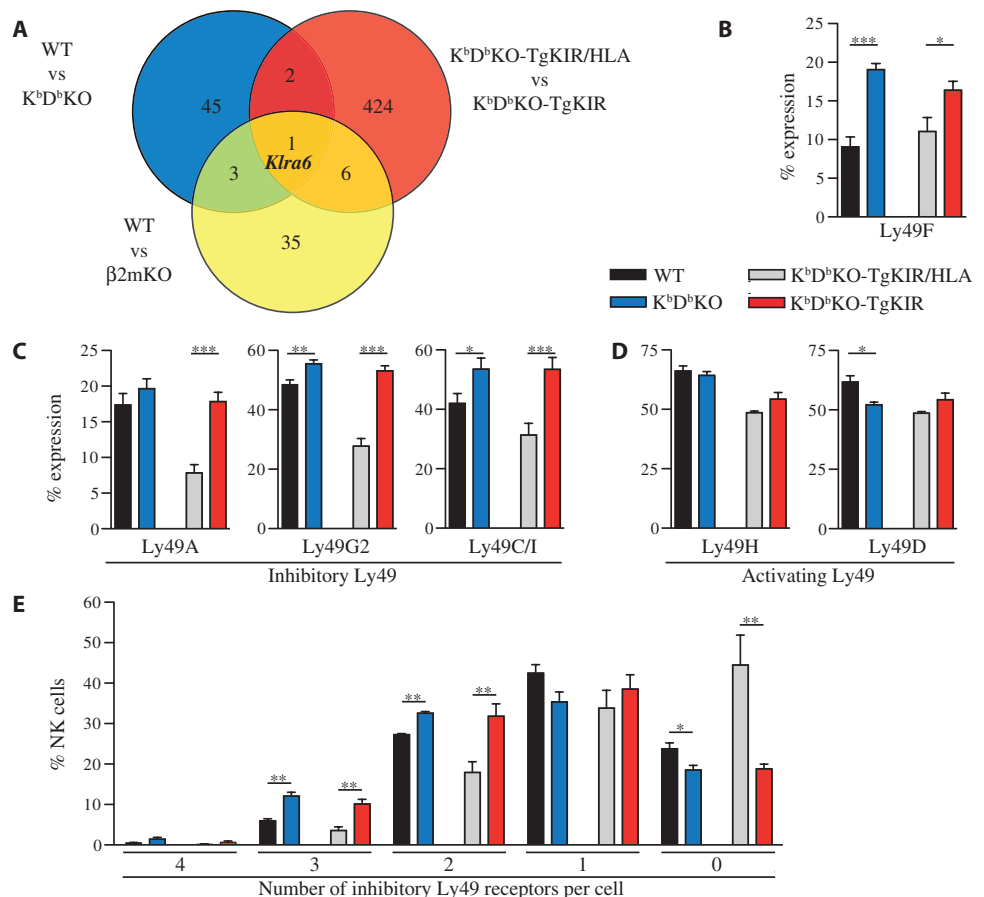
An increase in the percentage of NK cells in the hyporesponsive population that express each unbound Ly49 inhibitory receptor would be expected to increase the probability that a single NK cell could express multiple Ly49 inhibitory receptors. To test this, we analyzed the percentage of cells that had zero, one, two, three, or four inhibitory receptors. Consistent with our hypothesis, the percentage of NK cells that expressed more than one inhibitory receptor was higher within the hyporesponsive NK cell population than within the population of wild-type NK cells (Fig. 2E). Moreover, the fraction of NK cells that did not express any Ly49 inhibitory receptor was also reduced in the hyporesponsive NK cell population compared to that in wild-type NK cells. Thus, in the absence of detectable MHC class I molecules, NK cell tolerance was associated with the overrepresentation of a hyporesponsive NK cell population that had unbound, MHC class I-specific inhibitory receptors.

Expression of unbound Ly49 inhibitory receptors is related to NK cell hyporesponsiveness

The effect of self MHC class I on the skewing of the repertoire of inhibitory Ly49 receptors led us to directly analyze the consequences of these modifications on NK cell responsiveness. In wild-type mice, Ly49F⁺ cells produced little IFN- γ in response to stimulation of NK1.1 (Fig. 3A, upper panel). In contrast, KLRG1⁻ NK cells responded similarly to KLRG1⁺ NK cells (Fig. 3A, lower panel). Thus, even if the amounts of KLRG1 and Ly49F were modulated between the hyporesponsive and the competent NK cell populations (Figs. 1B and 2B), only Ly49F was associated with the reduced responsiveness of NK cells. This defect in the NK cell response was not because of a decrease in the abundance of NK1.1 at the cell surface. In addition, $72.5 \pm 5.9\%$ ($n = 5$) of Ly49F⁺ cells from wild-type mice also expressed Ly49C/I, NKG2A, or both, ruling out the possibility that these cells were hyporesponsive because of a lack of MHC class I-dependent education.

Because NK cells that expressed unbound Ly49 inhibitory receptors other than Ly49F were also overrepresented in the hyporesponsive NK cell population, we investigated the effects of these receptors on NK cell responsiveness in our two experimental mouse models. In our flow cytometric analysis of wild-type mice, we gated on competent Ly49C/I⁺ NK cells

Fig. 2. The education of NK cells is associated with few alterations in the NK transcriptional program and a skewing in the repertoire of Ly49 inhibitory receptors. (A) Microarray analysis of sorted splenic NK cells isolated from WT, K^bD^b KO, β 2mKO, K^bD^b KO-TgKIR/HLA, and K^bD^b KO-TgKIR mice. The blue circle contains genes that were differentially expressed, with a minimum of a factor of 1.7 change when comparing NK cells from WT mice with those from K^bD^b KO mice. The green circle shows differentially expressed genes with a minimum of a 1.7-fold change when comparing NK cells from WT mice to those from β 2mKO mice. The red circle shows differentially expressed genes with a minimum of a factor of 1.7 change when comparing NK cells from K^bD^b KO-TgKIR/HLA mice to those from K^bD^b KO-TgKIR mice. The intersection of the three circles indicates genes present in the indicated analysis that are likely to account for the transcriptional changes related to NK cell education. (B to E) Splenocytes were analyzed for the indicated cell surface markers by multiparametric flow cytometry. Results show the means \pm SEM. Statistical analysis was performed with the Mann-Whitney test. (B to D) Histograms display the expression of NK cell receptors on NK cells defined as NKp46⁺ aquadecad⁻ cells. (B and C) Data were pooled from at least six experiments. (D) Data were pooled from at least two independent experiments, with a total of three mice per group. (E) Splenocytes were incubated with antibodies against Ly49A, Ly49C/I, Ly49F, Ly49G2, NK1.1, CD19, and CD3, together with the aquadecad viability marker. Boolean analysis of inhibitory Ly49 receptor expression on NK cells



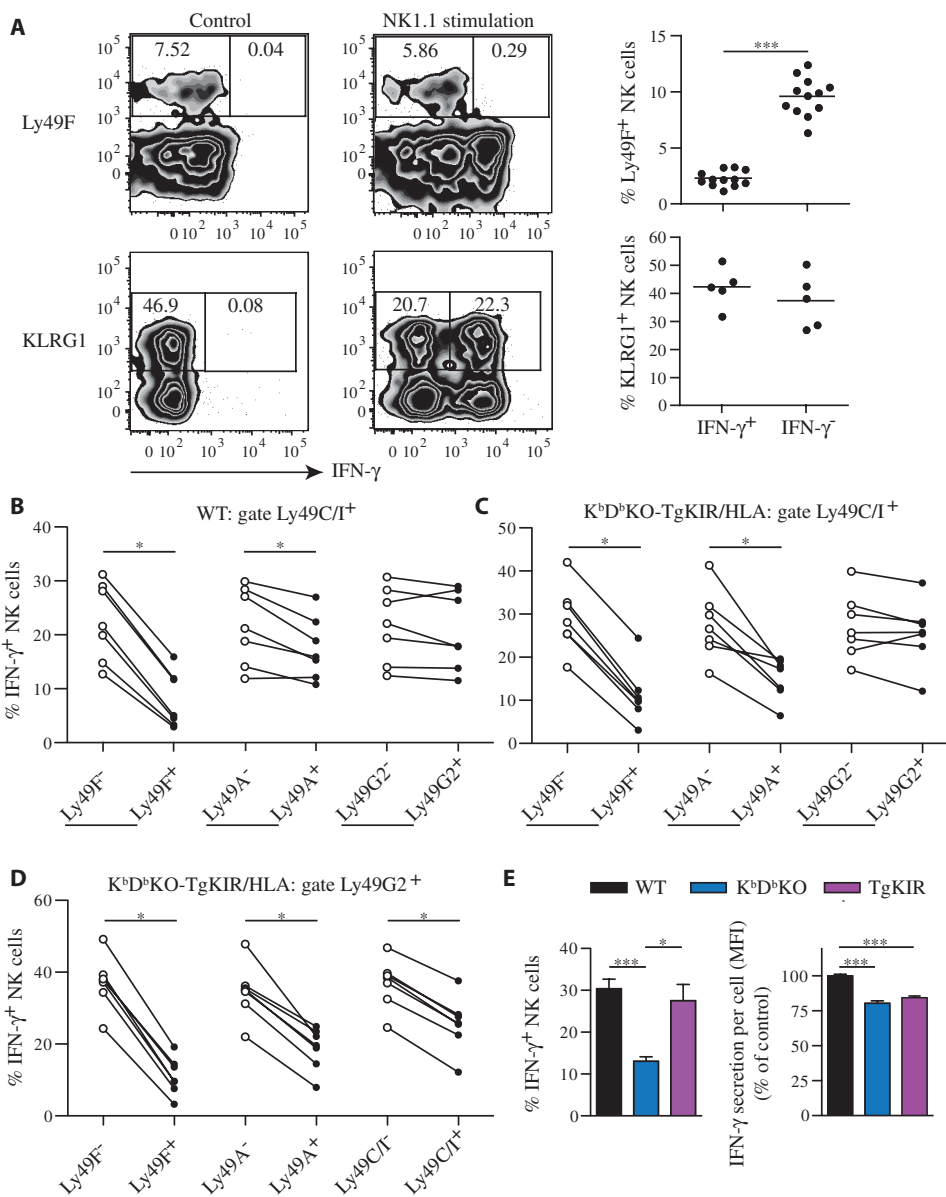
defined as NK1.1⁺CD19⁻CD3⁻aquadecad⁻ cells was performed (considering Ly49C/I as a single individual receptor). The frequencies of NK cells expressing from zero to four inhibitory Ly49 receptors per cell were computed. Data were pooled from four independent experiments, with a total of five mice per group. * $P < 0.05$; ** $P < 0.01$; *** $P < 0.001$.

and compared the percentages of IFN- γ ⁺ cells in NK cell subsets that had or did not have a given unbound Ly49 receptor. IFN- γ ⁺ NK cells were enriched in Ly49F⁻ NK cells, consistent with our earlier data (Fig. 3B). Similarly, Ly49A⁺ NK cells were less responsive than Ly49A⁻ NK cells (Fig. 3B). In our analysis of K^bD^bKO-TgKIR/HLA mice, in which all of the NK cells were educated through KIR-HLA interactions, we gated either on Ly49C/I⁺ (Fig. 3C) or on Ly49G2⁺ NK cells (Fig. 3D) to exclude any potential contamination by immature Ly49⁻ NK cells that could obscure the analysis. As for wild-type mice, we found that the presence of Ly49F and Ly49A was associated with a reduction in the percentage of IFN- γ -producing cells (Fig. 3C). The cell surface expression of unbound Ly49C/I was also associated with NK cell hyporesponsiveness in K^bD^bKO-TgKIR/HLA mice

(Fig. 3D). In contrast, the expression of Ly49G2 was not associated with changes in NK responsiveness (Fig. 3, B and C). Thus, the expression of unbound inhibitory Ly49 receptors was not equally associated with NK cell hyporesponsiveness, suggesting that there was some degree of specificity in the possible role of inhibitory receptors in the establishment of MHC class I-independent NK cell tolerance.

To further test this point, we assessed the function of NK cells isolated from transgenic mice expressing the human KIR2DL3 (TgKIR) on a wild-type background (Fig. 3E). Because KIR2DL3 selectively interacts with the human HLA allele Cw3 (7), all of the NK cells in this mouse expressed an unbound inhibitory receptor at their surface. Although the intensity of IFN- γ production per cell upon stimulation of NK1.1 (that is, the IFN- γ MFI

Fig. 3. Relationship between the expression of unbound inhibitory receptors and NK cell hyporesponsiveness. Multiparametric flow cytometry was performed on splenocytes isolated from WT, K^bD^bKO, K^bD^bKO-TgKIR/HLA, and K^bD^bKO-TgKIR mice. Each symbol represents an individual mouse. (A) WT splenocytes were stimulated for 4 hours in vitro on plates coated with NK1.1 mAb. Cells were then incubated with antibodies against the surface markers NKp46, Ly49F, or KLRG1, and with antibody against intracellular IFN- γ . (Left) Representative dot plots of Ly49F or KLRG1 against intracellular IFN- γ among NK cells after treatment with isotype control antibody (control) or antibody against NK1.1. (Right) Graphs show the frequencies of Ly49F⁺ ($n = 12$ mice from eight experiments) or KLRG1⁺ ($n = 5$ mice from two experiments) among IFN- γ ⁺ and IFN- γ ⁻ NK cell subsets after stimulation of NK1.1. NK cells were defined as NKp46⁺CD3⁻aquadead⁻ cells. *P* values were determined by Wilcoxon matched-pairs test. (B to D) WT and K^bD^bKO-TgKIR/HLA splenocytes were stimulated for 4 hours in vitro on plates coated with antibody against NK1.1. Cells were then incubated with antibodies against Ly49A, Ly49C/I, Ly49F, Ly49G2, NK1.1, CD19, and CD3, as well as the aqua dead viability marker. (B to D) Frequencies of IFN- γ ⁺ cells among Ly49C/I⁺ or Ly49G2⁺ NK cells expressing (closed circles) or not expressing (open circles) the indicated unbound Ly49 inhibitory receptors. Data are pooled from four experiments. *P* values were determined with the Wilcoxon matched-pairs test. (E) WT, K^bD^bKO, and TgKIR splenocytes were stimulated for 4 hours in vitro on plates coated with antibody against NK1.1. Intracellular IFN- γ production was measured in NK cells (NKp46⁺aquadead⁻). Data show the frequencies of IFN- γ ⁺ NK cells (left panel) and the amount of IFN- γ secreted per cell (MFI) (right panel). The IFN- γ MFIs of IFN- γ ⁺ NK cells isolated from K^bD^bKO and TgKIR mice were normalized to the value from WT mice to calculate the percentage compared to the control. Data were pooled from six experiments. Statistical analysis was performed with the Mann-Whitney test. **P* < 0.05; ****P* < 0.001.



among IFN- γ^+ cells) in TgKIR NK cells was lower relative to that in wild-type NK cells, the percentage of IFN- γ^+ TgKIR NK cells was comparable to that of IFN- γ^+ wild-type NK cells. Therefore, the transgenic expression of an unbound inhibitory receptor was sufficient to dampen the reactivity of NK cells, but not to an extent comparable to that induced under conditions of MHC class I-independent tolerance.

NK cell tolerance is associated with the confinement of activating receptors at the plasma membrane

Given that the overexpression of unbound inhibitory receptors did not fully account for the hyporesponsiveness of NK cells and that the global membrane density of activating receptors was identical in hyporesponsive and competent NK cells, we sought to analyze the ultrafine organization of these receptors at the membrane. Because of its sensitivity to low concentrations of fluorescent molecules, its noninvasiveness due to low intensity of excitation light requirement, and its data analysis robustness, the spot variable fluorescence correlation spectroscopy (svFCS) method was the most appropriate approach to study the dynamic membrane confinement of surface receptors in living cells (26–30). We therefore analyzed the dynamics of the organization of inhibitory and activating receptors by measuring the lateral diffusion, based on FCS analysis at different spatial scales of observation, of receptors present at the surface of hyporesponsive or competent NK cells. The transit time τ_d (that is, the average time that a fluorescent molecule stayed within the focal volume of observation) was measured at various focal volumes, which enabled us to plot the time-versus-area curve, namely, the FCS diffusion law. This is based on the fact that if molecules diffuse freely, one can expect that the average time (τ_d) that a molecule stays in a defined area is strictly proportional to the area of observation. In most situations in which diffusion is hindered, the FCS diffusion law no longer fits this scheme (31, 32). When permeable nanodomains are present, molecules partition dynamically into and out of the domains, the τ_d increases linearly with the area, and the intersection with the time axis (t_0) is positive. In a meshwork model, barriers impede the diffusion of membrane components. The molecules have a Brownian motion as long as they stay within the same mesh. When the radius, w , of observation is significantly larger than the size of the mesh, τ_d is an affine function of w^2 , with extrapolated t_0 being negative and its absolute value correlating directly with the average time that a molecule stays within a mesh.

We thus investigated whether the membrane confinement of inhibitory Ly49 molecules and activating NK1.1 proteins varied between hyporesponsive and competent NK cells. Because the increased abundance of Ly49C/I, Ly49A, and Ly49F is associated with NK cell hyporesponsiveness, and Ly49C/I is the most represented Ly49 receptor (fig. S2), we restricted our analysis to this inhibitory receptor. For Ly49C/I, we obtained similar t_0 values in wild-type and K^bD^b KO NK cells (-8.63 ± 13.9 and -16.00 ± 7.23 ms, respectively), which showed that the confinement of inhibitory molecules at the NK cell membrane was unchanged regardless of the educational status of the cell (Fig. 4A). The negative t_0 values suggested that this confinement was mainly dependent on a meshwork organization. In contrast, the confinement of NK1.1 varied greatly between competent and hyporesponsive NK cells. Indeed, NK1.1 had a t_0 value of 27.82 ± 6.27 ms in wild-type NK cells, whereas in K^bD^b KO NK cells, NK1.1 had a t_0 of -69.04 ± 7.05 ms (Fig. 4B). To assess whether this difference was directly linked to NK cell education, we studied the confinement of NK1.1 in NK cells upon NK cell education induced by the KIR-HLA interaction. In K^bD^b KO-TgKIR/HLA mice, the t_0 of NK1.1 was 33.22 ± 7.75 ms (Fig. 4B). Thus, NK1.1 activating receptors were confined differently depending on the educational status of the cells, whereas Ly49 inhibitory receptors were similarly confined in hyporesponsive and competent NK cells. That the t_0 values of NK1.1 were positive in competent NK cells and negative in hyporesponsive NK cells

suggested that the activating receptors were in nanodomains in competent NK cells, but in meshwork structures in hyporesponsive NK cells.

Next, we analyzed the membrane localization of another activating receptor, NKp46, in both competent and hyporesponsive NK cells. To rule out the possibility that the fluorescently labeled mAb fragments used to track NK1.1 or Ly49C/I receptors could interfere with our measurements, we generated an NKp46 knock-in mouse model (NKLT) in which an NKp46-enhanced green fluorescent protein (eGFP) fusion protein replaced the endogenous NKp46 protein (Fig. 5A and fig. S3). The expression of NKp46-eGFP corresponded to that of endogenous NKp46 (Fig. 5B). We restricted our analysis to that of NKLT $^{+/-}$ heterozygous knock-in mice to limit the contribution of the autofluorescence associated with the cells, a critical parameter for FCS measurements. The reactivity of freshly isolated

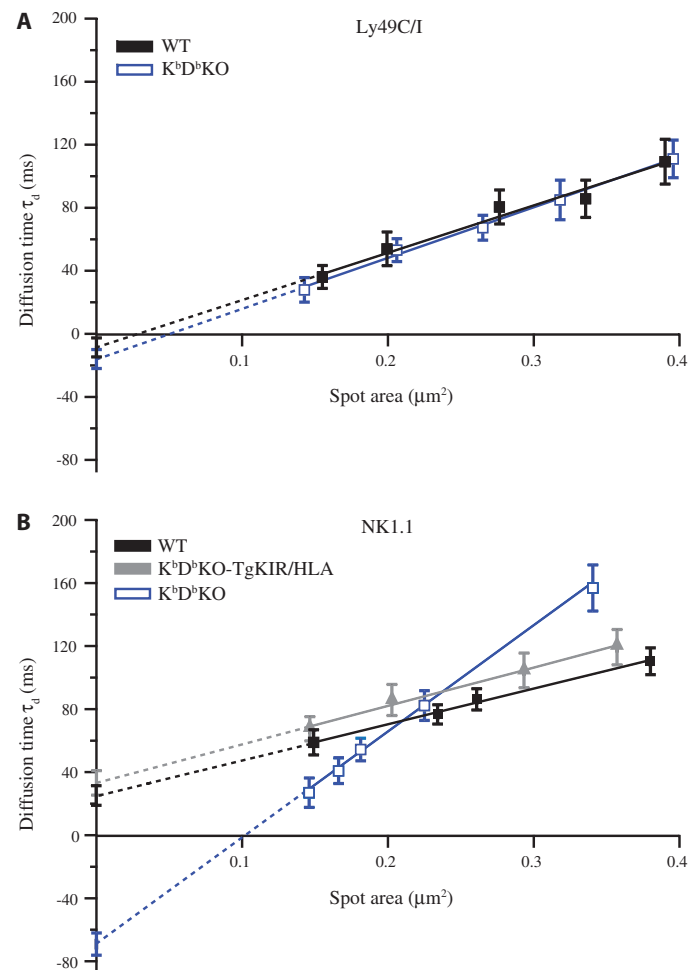


Fig. 4. NK cell responsiveness is associated with a modification in the membrane confinement of activating receptors. Receptor dynamics assessed by svFCS on living NK cells. Cells were marked with either fluorescent Fab against Ly49C/I or antibody against NK1.1. FCS diffusion laws were established for each receptor on WT, K^bD^b KO, and K^bD^b KO-TgKIR/HLA cells, and these were used to extrapolate the time intercept, t_0 . Data show the means \pm SD from 11 to 23 measurements. (A and B) FCS diffusion laws of Ly49C/I in WT and K^bD^b KO cells (A) and of NK1.1 in K^bD^b KO and K^bD^b KO-TgKIR/HLA cells (B). The spot area corresponds to the section of membrane that was excited by the laser beam.

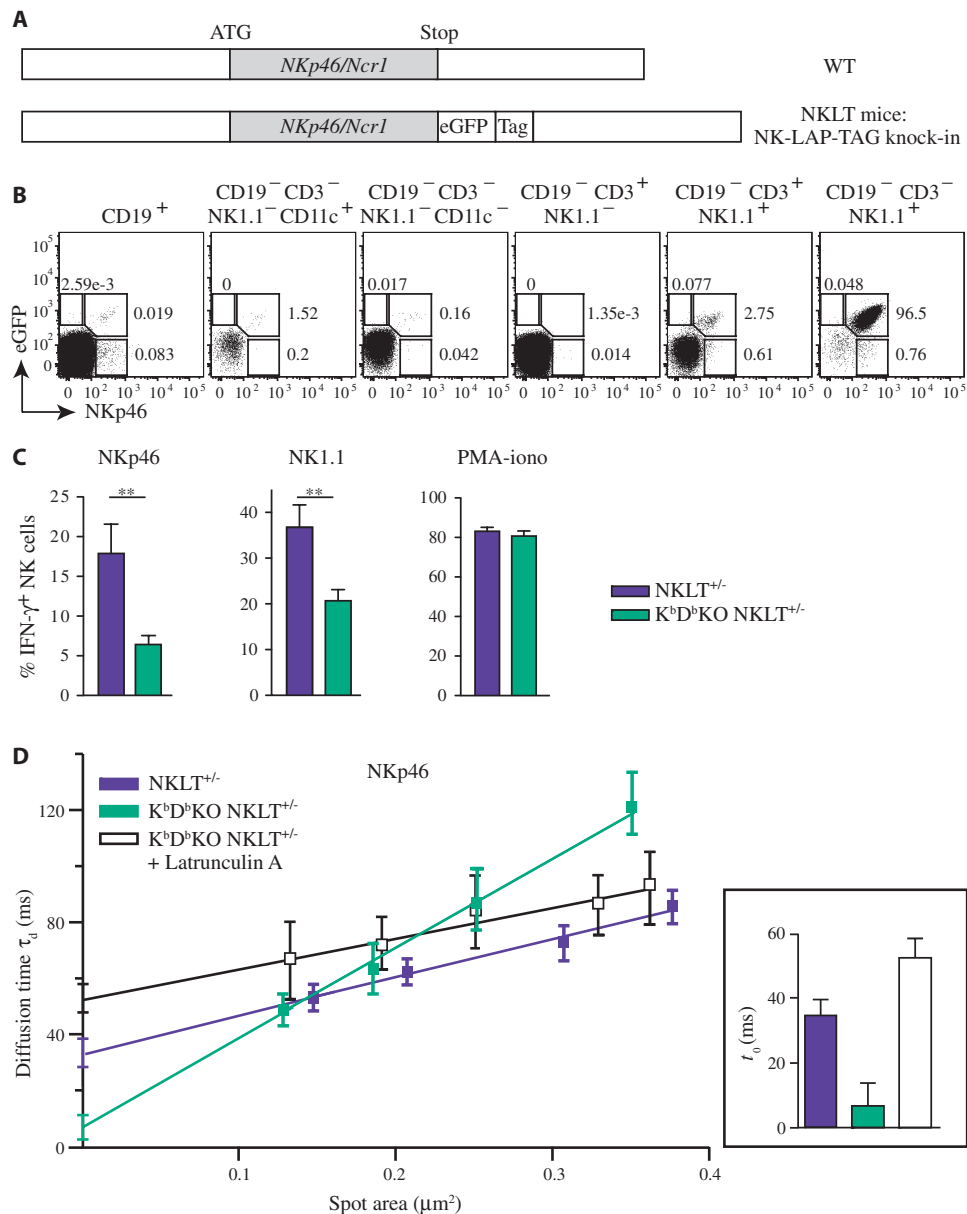


Fig. 5. Effects of NK cell education on the confinement of activating receptors. **(A)** Representative scheme of the *NKp46* locus in NKLT mice. NKp46 was fused to eGFP and a localization and affinity purification tag (LAP-TAG). **(B)** Expression of the NKp46-eGFP fusion protein in NKLT^{+/-} mice. eGFP and NKp46 are shown in B cell (CD19⁺), dendritic cell (CD19⁻CD3⁻NK1.1⁻CD11c⁺), lineage⁻, T cell (CD19⁻CD3⁺NK1.1⁻), NKT cell (CD19⁻CD3⁺NK1.1⁺), and NK cell (CD19⁻CD3⁻NK1.1⁺) types. **(C)** WT, NKLT^{+/-}, K^bD^bKO, and K^bD^bKO NKLT^{+/-} splenocytes were stimulated for 4 hours in vitro on plates coated with antibody against NKp46 or antibody against NK1.1. Maximal cell responsiveness was assessed by stimulation with phorbol 12-myristate 13-acetate (PMA) and ionomycin (iono). Intracellular IFN-γ production was measured in NK cells (NK1.1⁺ aquadead⁻ or NKp46⁺ aquadead⁻). Data show the frequencies of IFN-γ⁺ NK cells. **(D)** Receptor dynamics as assessed by svFCS on living NK cells. NKp46 was assessed directly by eGFP fluorescence. FCS diffusion laws were established for NKp46 and used to extrapolate the time intercept (t_0) in NKLT^{+/-}, K^bD^bKO NKLT^{+/-}, and latrunculin A-treated K^bD^bKO NKLT^{+/-} NK cells. Data show the means ± SD from 11 to 23 measurements. Inset: t_0 values of NKp46 diffusion laws in NKLT^{+/-}, K^bD^bKO NKLT^{+/-}, and latrunculin A-treated K^bD^bKO NKLT^{+/-} NK cells.

NKLT^{+/-} NK cells was comparable to that of wild-type NK cells (Fig. 5C), indicating that the eGFP fusion protein did not affect the activation of NK cells. NKLT mice were then crossed onto a K^bD^bKO background (K^bD^bKO NKLT^{+/-}) to analyze the confinement of NKp46 in the absence of MHC class I-dependent education. NK cells from K^bD^bKO NKLT^{+/-} mice were hyporesponsive upon stimulation of NK1.1 and NKp46 (Fig. 5C and fig. S4), confirming the validity of this model.

We found that NKp46 was confined differently at the membrane of competent (NKLT^{+/-}) and hyporesponsive (K^bD^bKO NKLT^{+/-}) NK cells. Indeed, NKp46 had a t_0 value of 34.28 ± 5.19 ms in NKLT^{+/-} NK cells, whereas its t_0 value decreased to 6.4 ± 7.5 ms in K^bD^bKO NKLT^{+/-} NK cells (Fig. 5D). Although NKp46 associated with membrane nanodomains in NKLT^{+/-} cells, consistent with the localization of NK1.1 in wild-type cells, the extent of the contribution of a meshwork structure to the confinement of NKp46 in hyporesponsive NK cells was less than that to the confinement of NK1.1 in K^bD^bKO cells. Therefore, we assessed the role of the actin cytoskeleton in the confinement of NKp46 in hyporesponsive NK cells in experiments with latrunculin A, which alters the actin-monomer subunit interface and specifically disrupts the actin cytoskeleton by preventing its polymerization (33). In K^bD^bKO NKLT^{+/-} NK cells treated with latrunculin A, the t_0 value of NKp46 was 51.8 ± 6.4 ms, as opposed to 6.4 ± 7.5 ms in untreated cells, indicating a major contribution of the actin-cytoskeleton to the confinement of this molecule at the membrane of hyporesponsive NK cells (Fig. 5D). Thus, with two independent NK cell receptors and two distinct strategies of fluorescent labeling, we showed that MHC class I-dependent NK cell education specifically altered the dynamic distribution of activating receptors at the plasma membrane. These receptors localized in nanodomains at the membrane of competent NK cells, whereas they were confined in actin-meshwork structures in hyporesponsive NK cells.

DISCUSSION

Great efforts have been made to understand the mechanisms of tolerance because loss of self-tolerance is closely related to the development of autoimmune diseases in animal models and humans. However, the pathways that lead to the induction of tolerance are not well elucidated, and the study of

tolerance has been mostly restricted to investigations of T and B cells. Here, we conducted a study to dissect the mechanisms that lead to NK cell tolerance when NK cells cannot detect self MHC class I molecules through inhibitory receptors, as well as the mechanisms by which the detection of self MHC class I through inhibitory receptors educates NK cells to become competent. The role of self MHC class I molecules in the education of NK cells was initially revealed by the hyporesponsiveness of NK cells raised in MHC class I-deficient mice relative to NK cells from wild-type mice (34–36). It was later demonstrated that this recognition of self MHC class I by inhibitory NK cell receptors governs the education of NK cells in humans and mice (10, 12, 37, 38). Here, we compared NK cells from wild-type mice with those from K^bD^b KO mice, NK cells from K^bD^b KO-TgKIR/HLA mice with those of K^bD^b KO-TgKIR mice, and NK cells from NKL $T^{+/-}$ mice with those of K^bD^b KO NKL $T^{+/-}$ mice to dissect the mechanisms responsible for the difference in NK cell reactivity in MHC class I-sufficient and -deficient backgrounds. Our results revealed that (i) MHC class I-dependent education of NK cells led to a skewing of the repertoire of inhibitory Ly49 molecules in the NK cell population, (ii) an increase in the abundance of unbound inhibitory receptors was not sufficient to fully account for the hyporesponsiveness of NK cells, and (iii) the membrane confinement of activating receptors was associated with NK cell tolerance and education. These results were obtained from experiments with three comparative pairs of mouse models, thus reinforcing the relevance of our findings.

We found that the hyporesponsiveness of the NK cell population was associated with an increased frequency of NK cells that expressed unbound MHC class I-specific receptors. This overrepresentation of Ly49 receptors was specific to inhibitory receptors because we observed no change in the abundances of Ly49 activating receptors. An increase in the frequency of NK cells that expressed inhibitory CD94-NKG2A heterodimers or KIR is observed in MHC class I-deficient patients (39–42), and NK cell education is thought to skew human NK cell repertoires (43). These findings are compatible with a model of NK cell development through which inhibitory MHC class I receptors are acquired sequentially (44). If the first MHC class I receptor expressed by an NK cell does not encounter its cognate ligand, then genes that encode other inhibitory receptors are sequentially

activated in the same cell, which leads to the cell surface expression of other potential inhibitory receptors for host MHC class I. Correspondingly, the interaction of inhibitory receptors with host MHC class I dampens further

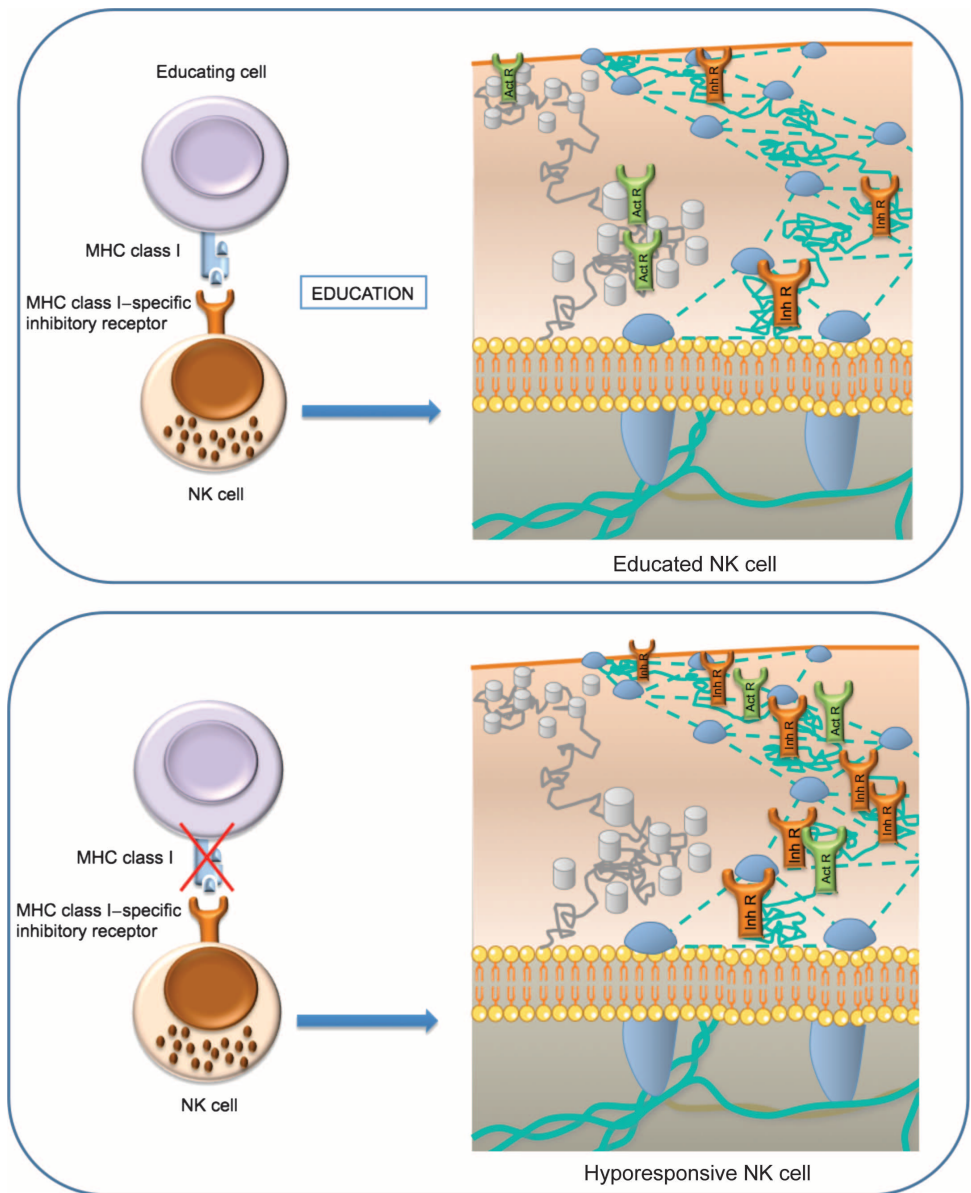


Fig. 6. Model of NK cell education. Plasma membranes from competent (**top**) and hyporesponsive (**bottom**) NK cells are schematically represented as yellow lipid bilayers with their extracytoplasmic (top layer) and intracytoplasmic surfaces (bottom layer). In MHC class I-educated NK cells, activating receptors (green) are confined in nanodomains (gray clusters), which are favorable zones for signaling. The lateral transport of activating receptors from nanodomain to nanodomain is represented as a gray line. In contrast, inhibitory MHC class I-specific receptors (red) are confined by a meshwork that is linked to the actin cytoskeleton (intracytoplasmic, turquoise lines). The lateral transport of inhibitory receptors is represented as a turquoise line at the surface of the plasma membrane. Cell surface receptors that are directly associated with the actin cytoskeleton are represented in blue. In the absence of MHC class I-dependent education, activating NK cell receptors (green) and inhibitory MHC class I-specific receptors (red) are confined in a meshwork that is linked to the actin cytoskeleton (turquoise lines).

expression of other inhibitory receptors. Our results thus favor the existence of a positive selection process that occurs during the development of NK cells, culminating in the preferential overrepresentation of NK cells that express inhibitory receptors specific for self MHC class I.

The association of NK cell hyporesponsiveness with the overrepresentation of NK cells that expressed unbound inhibitory receptors prompted us to test whether these receptors were directly responsible. This hypothesis was supported by data showing that unbound Ly49A can dampen the activation of NK cells (45). Our results showed that NK cells expressing the unbound inhibitory receptors Ly49A, Ly49C/I, and Ly49F were indeed less reactive than were NK cells that did not express these receptors. The effect was particularly strong for Ly49F; however, we did not observe any effect of Ly49G2. The molecular basis for the lack of association of Ly49G2 with NK cell hyporesponsiveness remains unclear because all of the Ly49 receptors are homologous. In addition, the transgenic expression of unbound inhibitory KIR only partially recapitulated NK cell hyporesponsiveness. The association of the expression of some, but not all, unbound inhibitory receptors and NK cell hyporesponsiveness could therefore result from a selective membrane organization that would favor their inhibitory function. Indeed, cell membranes show complex patterns of organization that result from either lipid-dependent (nanodomains) or cytoskeleton-based (meshwork) compartmentalizing forces (31).

Our nanoscopic analysis revealed that NK cell tolerance to MHC class I deficiency, and hence NK cell education to detect missing self, was associated with the confinement of activating receptors at the plasma membrane. In hyporesponsive NK cells, inhibitory and activating receptors were confined within an actin meshwork. In contrast, inhibitory and activating receptors in competent NK cells were confined by distinct geometrical membrane organizations; the former were diffused within a meshwork, whereas the latter were partitioned within nanodomains. It is possible that the confinement of activating and inhibitory receptors in the same membrane meshwork increases their likelihood of interacting with each other within the plasma membrane. Indeed, ITIM-bearing MHC class I-specific receptors require activating receptors to be in the vicinity to perform their inhibitory function (46). This possibility is consistent with our data that showed the association of the expression of unbound inhibitory receptors and NK cell hyporesponsiveness. Conversely, the localization of activating receptors in nanodomains of competent NK cells is consistent with the activation-prone status of these membrane structures, which are sensitive to cholesterol and sphingomyelin content, and are referred to as membrane rafts or islands (47, 48). Thus, we propose a model in which the engagement of inhibitory receptors specific for MHC class I regulates the confinement of activating receptors at the plasma membrane and thereby controls NK cell tolerance and education (Fig. 6).

The neutrophil Ly49Q receptor contributes, upon interaction with its MHC class I ligands, to the formation of membrane rafts in an ITIM- and SHP-2-dependent manner (49). The ITIM of Ly49A is critical in the establishment of NK cell education, but SHP-1 is not mandatory (13). Because inhibitory Ly49 receptors can recruit, upon tyrosine phosphorylation, both SHP-1 and SHP-2 (50), it is possible that SHP-2 is involved in the education of NK cells. Together, these findings support a model in which the sustained engagement of inhibitory receptors specific for MHC class I preferentially leads to the recruitment of SHP-2 and favors the association of activating NK cell receptors in nanodomains that are more favorable zones in which signaling can occur. An interruption in the triggering of inhibitory receptors would disrupt this maintenance of membrane compartmentalization. A continuous process of MHC class I-dependent education is consistent with the role of cis interactions of inhibitory receptors with MHC class I molecules (45). This scenario of NK cell education is also consistent with our gene profiling experiments that revealed few transcriptional differ-

ences between populations of competent and hyporesponsive NK cells. That NK cell education did not substantially alter the NK cell transcriptional program favors NK cell plasticity. Thus, competent and hyporesponsive NK cells might switch from one state to another. The plasticity of NK cell responsiveness could result from the constant detection of the amount of host MHC class I molecules by inhibitory receptors. This possibility is supported by data that showed that NK cells expressing inhibitory receptors can revert from a hyporesponsive to a competent status upon exposure to cognate MHC class I molecules (51, 52). Our findings thus position the cell surface confinement of activating receptors as a pivotal element of NK cell education, and they offer a different perspective on the role of ITIM-bearing receptors by showing that they can regulate the organization of the plasma membrane and thereby control tolerance.

MATERIALS AND METHODS

Mice

All mice were from a C57BL/6J background and were bred and maintained at the Centre d'Immunologie de Marseille-Luminy (CIML) animal facilities in specific pathogen-free conditions. K^bD^b KO mice were provided by F. Lemonier (Pasteur Institute, Paris). K^bD^b KO-TgHLA-Cw3 (K^bD^b KO-TgHLA), K^bD^b KO-TgKIR2DL3 (K^bD^b KO-TgKIR), K^bD^b KO-TgKIR/HLA, and TgKIR2DL3 (TgKIR) transgenic mice were previously described (20).

Generation of NKLT mice

A genomic fragment containing all *NCR1* exons into a bacterial artificial chromosome (BAC) clone (clone number RP23-106A10; Imagenes) was selected. Through Red/ET cloning (Gene Bridges), a 6.6-kb fragment containing the entire exon 7 of *NCR1* and centered on the stop codon was subcloned into the low copy plasmid pACYC177 and flanked with Sal I sites. Briefly, the following primers containing 85-nucleotide (nt) homology with *NCR1* were used to amplify PACYC177 by PCR: 5'-AATATGATTAGAATATTGTATGCAATCTCAATTAATAAAAATTTAAAAAATGAAGCTAGTCCACACAA-GTGTTCATTAATTGACGTCGACGGCTAGCGGAGTGTAATACTGGC-3', and 5'-AATAAGAAAAGCAGCTGATAGAGTAAGCTAATTGAGTCTTTCAGTCCAATGCCAGATCTCTTTAGCATTTTGTGATACTATGTCGACTGAAGACGAAAGGGCCTCGTG-3'. Restriction sites are in bold, whereas sequences with homology to the plasmid sequence are underlined. Competent DH5 α bacteria containing a plasmid encoding phage recombinase and the BAC were transformed with the PCR product by electroporation. Recombination events were screened by PCR. Next, we constructed a modification cassette in silico, consisting of an *NKp46*-tagging cassette and a selection cassette flanked by two 500-nt arms homologous to exon 7 of *NKp46* exon 7, either upstream or downstream of the stop codon. The tagging cassette was previously described (53), and it enables both the localization and the affinity purification of modified proteins with two different tags and protease cleavage sites, which enables the elution of immunoprecipitated complexes. The tagging cassette consists of (in order) a tobacco etch virus (TEV) protease cleavage site, the S-peptide (for affinity purification), the PreScission protease cleavage site, and eGFP for both localization and purification. The selection cassette, autoexcisable in vivo, has also been previously described and consists of loxP-tACE-CRE-PGK-gb2-neo-loxP. The whole modification cassette was synthesized (GeneArt) and used to modify the BAC subclone by homologous E/T recombination in bacteria. Recombination events were screened by PCR. After electroporation of Bruce 4 C57BL/6 embryonic stem (ES) cells and selection in G418, colonies were screened for homologous recombination by PCR analysis and

Southern blotting. The occurrence of an appropriate homologous recombination event at the 5' side was screened by PCR with the following nucleotides: 5'-CCCACACACACATCATAGAAAAG-3' (forward primer); 5'-CTTTATCCAGGTACAGCATAGAGC-3' (reverse primer, 3 kb, with wild-type allele); 5'-ACTGGGTGCTCAGGTAGTGGTT-3' (reverse primer, 3.8 kb, with knock-in allele). Next, a Southern blot with 3' and 5' probes was performed for some ES clones to further verify the recombination events. The 5' and 3' probes were obtained by PCR and tested on DNA digested with Bam HI (fig. S3A). A neomycin-specific probe was used to ensure that adventitious nonhomologous recombination events had not occurred in the selected clones. Mutant ES cells were injected into mouse blastocysts from the FVB strain. Germline transmission led to the self-excision of the selection cassette in male germinal cells. Screening of mice for the presence of the *NKLT* mutation was performed by PCR with the following oligonucleotides: 5'-TCGAATTGGTCTGGCATGCATAATC-3' (forward primer); 5'-GAGCACTTGTGCTCCTCCAGACAA-3' (reverse primer for the wild-type allele); and 5'-GTTCGAATTTAG-CAGCAGCGGTTTC-3' (reverse primer for the knock-in allele). This pair of primers amplifies a 546-base pair (bp) fragment in the case of the wild-type allele, and a 268-bp band in the case of the *NKLT* allele.

Antibodies

Purified antibody against Ly49C/I (5E6) was provided by Innate-Pharma. Purified antibodies against NKp46 (29A1.4) and against NK1.1 (PK136) were prepared by the CIML Monoclonal Antibody Facility. Antibodies against NKp46 and Ly49C/I were labeled with Alexa Fluor 647 according to the manufacturer's instructions (Invitrogen). Similarly, antibody against NK1.1 was labeled with Alexa Fluor 488 (Invitrogen). PerCP-Cy5.5-conjugated antibody against NKp46 (29A1.4); allophycocyanin (APC)-, biotin-, or PerCP-Cy5.5-conjugated antibody against NK1.1 (PK136); phycoerythrin (PE)- or APC-conjugated antibody against CD49b (DX5); fluorescein isothiocyanate (FITC)- or PerCP-Cy5.5-conjugated antibody against CD3 (145-2C11); PE-, APC-, or PE-Cy7-conjugated antibody against IFN- γ (XMG1.2); APC-conjugated antibody against KLRG1 (2F1); biotin- or FITC-conjugated antibody against NKG2A/C/E (20d5); biotin- or FITC-conjugated antibody against Ly49C/I (5E6); FITC-conjugated antibody against Ly49D (4E5); FITC-, PE-Cy7-, or APC-conjugated antibody against Ly49G2 (4D11); PE-conjugated antibody against Ly49F (HBF-719); Alexa Fluor 700-conjugated antibody against CD3 (500A2); APC-H7-conjugated antibody against CD19 (1D3); PerCP-Cy5.5-conjugated streptavidin; Pacific Blue-conjugated antibody against Ly49A (YE1/48.10.6); Alexa Fluor 647-conjugated antibody against Ly49H (3D10); and biotin-conjugated antibody against NKG2D (CX5) were obtained from BD Biosciences, Biolegend, or eBiosciences. Sample analysis was performed on a FACSCanto II, LSR, or LSR II flow cytometers (BD Biosciences) with FACSDiva software. Results were analyzed with FlowJo software (Tree Star). NK cells were defined in the gate of lymphocytes depending on the parameters for size and granulometric as defined by side scatter (SSC) and forward scatter (FSC).

Cell isolation and culture

Splenocyte suspensions were obtained by mechanical disruption of mouse spleen on a 70- μ m cell strainer (BD Biosciences) in complete medium. Red blood cells were lysed by hypotonic buffer with 0.16 M NH_4Cl and 17 mM tris-HCl (pH 7.2). NK cells were enriched by negative depletion with mAbs against CD4, CD5, CD8, Ter119, and IA/IE, as previously described (54). NK cell purity was assessed by flow cytometry to be 80 to 90%. Hybridoma supernatant containing antibody against Fc γ R2/III (2.4G2) that was used to block Fc receptors was produced in the laboratory. Isolated NK cells were used for Ca^{2+} flux measurement, cell sorting, confocal microscopy, and FCS measurements.

Measurement of Ca^{2+} flux

All steps, including the preparation of NK cells, were performed at room temperature in Hanks' balanced salt solution (HBSS with Ca^{2+} and Mg^{2+} , without phenol red; #415-008, PAA) containing 1% fetal calf serum. Isolated NK cells (10^7 cells/ml) were loaded for 1 hour at 37°C with Indo-1/AM (5 μ M final concentration; #402096, Calbiochem). Cells were washed and then incubated with FITC-conjugated antibody against CD3 and APC-conjugated antibody against CD49b in the presence of 2.4G2. Before sample acquisition, each tube (10^6 cells/ml) was prewarmed at 37°C for a few minutes. As a positive control, cells were stimulated with ionomycin (1 μ g/ml, Sigma) to obtain maximal responses. For specific activation, biotin-conjugated antibodies against NK1.1 or NKG2D were added (at a final concentration of 2.5 μ g/ml) followed by ImmunoPure streptavidin (5 μ g/ml; Pierce). Changes in intracellular Ca^{2+} over the time were monitored with the Indo-1 (violet) and Indo-1 (blue) channels on an LSR or LSR II flow cytometer with CellQuest or FACSDiva software. Results were analyzed with FlowJo software.

Cell sorting

Isolated NK cells were incubated with FITC-conjugated antibody against CD3 and APC-conjugated antibody against NK1.1 in the presence of 2.4G2. Cells were washed and then resuspended at 10^7 cells/ml in phosphate-buffered saline (PBS) containing 2% fetal calf serum and 2 mM EDTA. After the addition of propidium iodide (1 μ g/ml, Sigma), NK cells were sorted on a FACS Vantage flow cytometer (BD Biosciences). NK cell purity was assessed by flow cytometry to be 96 to 99%.

Measurement of IFN- γ production

Splenocyte suspensions were distributed in a 96-well 2HB Immulon plate precoated with antibody against NK1.1 (25 μ g/ml) or antibody against NKp46 (10 μ g/ml). Cells were activated in the presence of monensin (GolgiStop; BD Biosciences) or, alternatively, brefeldin A (eBiosciences) in complete medium [RPMI 1640 (Gibco/Invitrogen) supplemented with 10% fetal calf serum, 1 mM sodium pyruvate, 10 mM Hepes, penicillin (100 U/ml), and streptomycin (100 μ g/ml)]. After 4 hours at 37°C, cell surface staining was performed, which included the use of a fixable aqua dead cell dye (Invitrogen, Molecular Probes) to test for cell viability. For intracellular IFN- γ staining, cells were fixed with 2% paraformaldehyde (PFA) and permeabilized with Perm/Wash solution (BD Pharmingen).

RNA extraction and microarray analysis

Total RNA was extracted with the RNeasy Micro Kit (Qiagen) from sorted splenic NK cells ($\text{NK1.1}^+\text{CD3}^-$) isolated from wild-type, $\text{K}^{\text{b}}\text{D}^{\text{b}}\text{KO}$, $\beta 2\text{mKO}$, $\text{K}^{\text{b}}\text{D}^{\text{b}}\text{KO-TgKIR/HLA}$, and $\text{K}^{\text{b}}\text{D}^{\text{b}}\text{KO-TgKIR}$ mice. The purity of cells was more than 97%. The quality of the RNA and the absence of genomic DNA contamination were assessed with Bioanalyzer (Agilent Technologies). RNA from each sample was processed by Ipsogen and hybridized to Affymetrix murine genome microarray chips 430.2.0. Data obtained were analyzed with GeneSpring software (GX 10 version). Data were first normalized and filtered by percentile (upper cutoff, 100; lower cutoff, 20). Differentially expressed genes were then identified with an unpaired *t* test ($P < 0.05$) followed by a fold-change filter with a cutoff of 1.7. This analysis was performed independently on the three models: (i) data from wild-type cells were compared to those from $\text{K}^{\text{b}}\text{D}^{\text{b}}\text{KO}$ NK cells, (ii) data from wild-type cells were compared to those from $\beta 2\text{mKO}$ NK cells, and (iii) data from $\text{K}^{\text{b}}\text{D}^{\text{b}}\text{KO-TgKIR/HLA}$ were compared to those from $\text{K}^{\text{b}}\text{D}^{\text{b}}\text{KO-TgKIR}$ NK cells. Candidate gene lists from each analysis were then crossed to identify genes found in common in both models.

Fab production and svFCS measurements

Monovalent antibody fragments (Fabs) were prepared by papain digestion of Ly49C/I and NK1.1 mAbs. Fast protein liquid chromatography (FPLC)-purified Fabs were conjugated with Alexa Fluor 488 with the Alexa Fluor 488 Antibody Labeling Kit (Invitrogen), to get on average about one dye per molecule. Freshly isolated NK cells were seeded at a low density on poly-L-lysine-coated coverslips. Cells were then incubated in complete medium in the presence of the fluorescently labeled Fabs for 15 min, and then gently washed twice in HBSS and 10 mM Hepes (pH 7.4). FCS measurements were immediately performed at 37°C on a custom-made apparatus based on a confocal-based Axiovert 200M microscope (Zeiss) with an excitation 488-nm argon ion laser beam focused through a C-Apochromat 40×, NA (numerical aperture) 1.2 objective. The laser waist w was set by a diaphragm that altered the lateral extension of the laser beam falling onto the back aperture of the microscope objective (32). Fluorescence was collected through a 545/20-nm band-pass filter. Autocorrelations were processed by a hardware correlator (Correlator.com), and the data were analyzed with built-in functions of IGOR Pro (WaveMetrics). The FCS diffusion laws were established from four to five different waists, with each value as the average of 12 to 23 measurements on at least seven different cells. The diffusion time τ_d , defined as the lag time at half-maximum autocorrelation function (ACF), was based on 20 independent runs of 5 s for Ly49C/I and 10 s for NK1.1 and NKp46. For treatment with latrunculin A, NK cells were preincubated for 5 min in HBSS containing EDTA and latrunculin A (1 μ M), and then FCS was performed in HBSS containing EDTA and latrunculin A (0.1 μ M).

Statistical analysis

All P values were determined with Prism software (GraphPad Software Inc.) using nonparametric unpaired or paired tests (two-tailed) as indicated. P values below 0.05 were considered significant and were designated in figures as follows: * P < 0.05; ** P < 0.01; *** P < 0.001.

SUPPLEMENTARY MATERIALS

www.sciencesignaling.org/cgi/content/full/4/167/ra21/DC1

Fig. S1. NK cell education affects proximal signaling.

Fig. S2. Surface expression of NK cell receptors.

Fig. S3. Generation and identification of NKLT mice.

Fig. S4. Responsiveness of NKLT^{+/−} NK cells.

Table S1. Lists of probe sets differentially expressed in NK cells from K^DP⁰KO-TgKIR/HLA and K^DP⁰KO-TgKIR mice.

Table S2. Lists of probe sets differentially expressed in NK cells from wild-type and K^DP⁰KO mice.

Table S3. Lists of probe sets differentially expressed in NK cells from wild-type and β 2mKO mice.

REFERENCES AND NOTES

- H. von Boehmer, F. Melchers, Checkpoints in lymphocyte development and autoimmune disease. *Nat. Immunol.* **11**, 14–20 (2010).
- E. Vivier, E. Tomasello, M. Baratin, T. Walzer, S. Ugolini, Functions of natural killer cells. *Nat. Immunol.* **9**, 503–510 (2008).
- E. Vivier, D. H. Raulet, A. Moretta, M. A. Caligiuri, L. Zitvogel, L. L. Lanier, W. M. Yokoyama, S. Ugolini, Innate or adaptive immunity? The example of natural killer cells. *Science* **331**, 44–49 (2011).
- L. L. Lanier, NK cell recognition. *Annu. Rev. Immunol.* **23**, 225–274 (2005).
- E. O. Long, Regulation of immune responses through inhibitory receptors. *Annu. Rev. Immunol.* **17**, 875–904 (1999).
- E. Vivier, J. A. Nunès, F. Vély, Natural killer cell signaling pathways. *Science* **306**, 1517–1519 (2004).
- A. Moretta, C. Bottino, M. Vitale, D. Pende, R. Biassoni, M. C. Mingari, L. Moretta, Receptors for HLA class-I molecules in human natural killer cells. *Annu. Rev. Immunol.* **14**, 619–648 (1996).
- W. M. Yokoyama, W. E. Seaman, The Ly-49 and NKR-P1 gene families encoding lectin-like receptors on natural killer cells: The NK gene complex. *Annu. Rev. Immunol.* **11**, 613–635 (1993).
- D. H. Raulet, N. Guerra, Oncogenic stress sensed by the immune system: Role of natural killer cell receptors. *Nat. Rev. Immunol.* **9**, 568–580 (2009).
- N. Anfossi, P. André, S. Guia, C. S. Falk, S. Roetyncck, C. A. Stewart, V. Bresò, C. Frassati, D. Reviron, D. Middleton, F. Romagné, S. Ugolini, E. Vivier, Human NK cell education by inhibitory receptors for MHC class I. *Immunity* **25**, 331–342 (2006).
- P. Brodin, T. Lakshminanth, S. Johansson, K. Kärre, P. Höglund, The strength of inhibitory input during education quantitatively tunes the functional responsiveness of individual natural killer cells. *Blood* **113**, 2434–2441 (2009).
- N. C. Fernandez, E. Treiner, R. E. Vance, A. M. Jamieson, S. Lemieux, D. H. Raulet, A subset of natural killer cells achieves self-tolerance without expressing inhibitory receptors specific for self-MHC molecules. *Blood* **105**, 4416–4423 (2005).
- S. Kim, J. Poursine-Laurent, S. M. Truscott, L. Lybarger, Y. J. Song, L. Yang, A. R. French, J. B. Sunwoo, S. Lemieux, T. H. Hansen, W. M. Yokoyama, Licensing of natural killer cells by host major histocompatibility complex class I molecules. *Nature* **436**, 709–713 (2005).
- D. H. Raulet, R. E. Vance, Self-tolerance of natural killer cells. *Nat. Rev. Immunol.* **6**, 520–531 (2006).
- W. M. Yokoyama, S. Kim, How do natural killer cells find self to achieve tolerance? *Immunity* **24**, 249–257 (2006).
- P. Parham, K. L. McQueen, Alloreactive killer cells: Hindrance and help for haematopoietic transplants. *Nat. Rev. Immunol.* **3**, 108–122 (2003).
- C. C. Stebbins, C. Watzl, D. D. Billadeau, P. J. Leibson, D. N. Burshtyn, E. O. Long, Vav1 dephosphorylation by the tyrosine phosphatase SHP-1 as a mechanism for inhibition of cellular cytotoxicity. *Mol. Cell Biol.* **23**, 6291–6299 (2003).
- M. E. Peterson, E. O. Long, Inhibitory receptor signaling via tyrosine phosphorylation of the adaptor Crk. *Immunity* **29**, 578–588 (2008).
- M. T. Orr, W. J. Murphy, L. L. Lanier, 'Unlicensed' natural killer cells dominate the response to cytomegalovirus infection. *Nat. Immunol.* **11**, 321–327 (2010).
- C. Sola, P. André, C. Lemmers, N. Fuseri, C. Bonnafous, M. Bléry, N. R. Wagtmann, F. Romagné, E. Vivier, S. Ugolini, Genetic and antibody-mediated reprogramming of natural killer cell missing-self recognition in vivo. *Proc. Natl. Acad. Sci. U.S.A.* **106**, 12879–12884 (2009).
- L. Corral, T. Hanke, R. E. Vance, D. Cado, D. H. Raulet, NK cell expression of the killer cell lectin-like receptor G1 (KLRG1), the mouse homolog of MAFA, is modulated by MHC class I molecules. *Eur. J. Immunol.* **30**, 920–930 (2000).
- C. Gründemann, S. Schwartzkopf, M. Koschella, O. Schweier, C. Peters, D. Voehringer, H. Pircher, The NK receptor KLRG1 is dispensable for virus-induced NK and CD8⁺ T-cell differentiation and function in vivo. *Eur. J. Immunol.* **40**, 1303–1314 (2010).
- K. Natarajan, N. Dimasi, J. Wang, R. A. Mariuzza, D. H. Margulies, Structure and function of natural killer cell receptors: Multiple molecular solutions to self, nonself discrimination. *Annu. Rev. Immunol.* **20**, 853–885 (2002).
- T. Hanke, H. Takizawa, C. W. McMahon, D. H. Busch, E. G. Pamer, J. D. Miller, J. D. Altman, Y. Liu, D. Cado, F. A. Lemonnier, P. J. Bjorkman, D. H. Raulet, Direct assessment of MHC class I binding by seven Ly49 inhibitory NK cell receptors. *Immunity* **11**, 67–77 (1999).
- J. Michaëlsson, A. Achour, M. Salcedo, A. Kåse-Sjöström, J. Sundbäck, R. A. Harris, K. Kärre, Visualization of inhibitory Ly49 receptor specificity with soluble major histocompatibility complex class I tetramers. *Eur. J. Immunol.* **30**, 300–307 (2000).
- D. Marguet, P. F. Lenne, H. Rigneault, H. T. He, Dynamics in the plasma membrane: How to combine fluidity and order. *EMBO J.* **25**, 3446–3457 (2006).
- K. Chakrabandhu, Z. Hérics, S. Huaault, B. Dost, L. Peng, F. Conchonaud, D. Marguet, H. T. He, A. O. Hueber, Palmitoylation is required for efficient Fas cell death signaling. *EMBO J.* **26**, 209–220 (2007).
- R. Lasserre, X. J. Guo, F. Conchonaud, Y. Hamon, O. Hawchar, A. M. Bernard, S. M. Soudja, P. F. Lenne, H. Rigneault, D. Olive, G. Bismuth, J. A. Nunès, B. Payrastra, D. Marguet, H. T. He, Raft nanodomains contribute to Akt/PKB plasma membrane recruitment and activation. *Nat. Chem. Biol.* **4**, 538–547 (2008).
- C. Eggeling, C. Ringemann, R. Medda, G. Schwarzmann, K. Sandhoff, S. Polyakova, V. N. Belov, B. Hein, C. von Middendorff, A. Schönle, S. W. Hell, Direct observation of the nanoscale dynamics of membrane lipids in a living cell. *Nature* **457**, 1159–1162 (2009).
- H. T. He, D. Marguet, Detecting nanodomains in living cell membrane by fluorescence correlation spectroscopy. *Annu. Rev. Phys. Chem.*, 10.1146/annurev-physchem-032210-103402 (2010).
- P. F. Lenne, L. Wawrezynieck, F. Conchonaud, O. Wurtz, A. Boned, X. J. Guo, H. Rigneault, H. T. He, D. Marguet, Dynamic molecular confinement in the plasma membrane by microdomains and the cytoskeleton meshwork. *EMBO J.* **25**, 3245–3256 (2006).
- L. Wawrezynieck, H. Rigneault, D. Marguet, P. F. Lenne, Fluorescence correlation spectroscopy diffusion laws to probe the submicron cell membrane organization. *Biophys. J.* **89**, 4029–4042 (2005).
- W. M. Morton, K. R. Ayscough, P. J. McLaughlin, Latrunculin alters the actin-monomer subunit interface to prevent polymerization. *Nat. Cell Biol.* **2**, 376–378 (2000).
- P. Höglund, R. Glas, C. Ohlen, H. G. Ljunggren, K. Karre, Alteration of the natural killer repertoire in H-2 transgenic mice: Specificity of rapid lymphoma cell clearance determined by the H-2 phenotype of the target. *J. Exp. Med.* **174**, 327–334 (1991).
- J. R. Dorfman, D. H. Raulet, Major histocompatibility complex genes determine natural killer cell tolerance. *Eur. J. Immunol.* **26**, 151–155 (1996).

36. P. Höglund, C. Ohlén, E. Carbone, L. Franksson, H. G. Ljunggren, A. Latour, B. Koller, K. Kärre, Recognition of β_2 -microglobulin-negative (β_2m^-) T-cell blasts by natural killer cells from normal but not from β_2m^- mice: Nonresponsiveness controlled by β_2m^- bone marrow in chimeric mice. *Proc. Natl. Acad. Sci. U.S.A.* **88**, 10332–10336 (1991).
37. S. Cooley, F. Xiao, M. Pitt, M. Gleason, V. McCullar, T. L. Bergemann, K. L. McQueen, L. A. Guethlein, P. Parham, J. S. Miller, A subpopulation of human peripheral blood NK cells that lacks inhibitory receptors for self-MHC is developmentally immature. *Blood* **110**, 578–586 (2007).
38. H. J. Kim, W. S. Min, Y. J. Kim, D. W. Kim, J. W. Lee, C. C. Kim, Haplotype mismatched transplantation using high doses of peripheral blood CD34⁺ cells together with stratified conditioning regimens for high-risk adult acute myeloid leukemia patients: A pilot study in a single Korean institution. *Bone Marrow Transplant.* **35**, 959–964 (2005).
39. H. Furukawa, T. Yabe, K. Watanabe, R. Miyamoto, A. Miki, T. Akaza, K. Tadokoro, S. Tohma, T. Inoue, K. Yamamoto, T. Juji, Tolerance of NK and LAK activity for HLA class I-deficient targets in a TAP1-deficient patient (bare lymphocyte syndrome type I). *Hum. Immunol.* **60**, 32–40 (1999).
40. G. Markel, H. Mussaffi, K. L. Ling, M. Salio, S. Gadola, G. Steuer, H. Blau, H. Achdout, M. de Miguel, T. Gonen-Gross, J. Hanna, T. I. Amon, U. Qimron, I. Volovitz, L. Eisenbach, R. S. Blumberg, A. Porgador, V. Cerundolo, O. Mandelboim, The mechanisms controlling NK cell autoreactivity in TAP2-deficient patients. *Blood* **103**, 1770–1778 (2004).
41. M. Vitale, J. Zimmer, R. Castriconi, D. Hanau, L. Donato, C. Bottino, L. Moretta, H. de la Salle, A. Moretta, Analysis of natural killer cells in TAP2-deficient patients: Expression of functional triggering receptors and evidence for the existence of inhibitory receptor(s) that prevent lysis of normal autologous cells. *Blood* **99**, 1723–1729 (2002).
42. J. Zimmer, L. Donato, D. Hanau, J. P. Cazenave, M. M. Tongio, A. Moretta, H. de la Salle, Activity and phenotype of natural killer cells in peptide transporter (TAP)-deficient patients (type I bare lymphocyte syndrome). *J. Exp. Med.* **187**, 117–122 (1998).
43. M. Yawata, N. Yawata, M. Draghi, F. Partheniou, A. M. Little, P. Parham, MHC class I-specific inhibitory receptors and their ligands structure diverse human NK-cell repertoires toward a balance of missing self-response. *Blood* **112**, 2369–2380 (2008).
44. C. Roth, J. R. Carlyle, H. Takizawa, D. H. Raulet, Clonal acquisition of inhibitory Ly49 receptors on developing NK cells is successively restricted and regulated by stromal class I MHC. *Immunity* **13**, 143–153 (2000).
45. A. Chalifour, L. Scarpellino, J. Back, P. Brodin, E. Devèvre, F. Gros, F. Lévy, G. Leclercq, P. Höglund, F. Beermann, W. Held, A role for cis interaction between the inhibitory Ly49A receptor and MHC class I for natural killer cell education. *Immunity* **30**, 337–347 (2009).
46. M. Bléry, J. Delon, A. Trautmann, A. Cambiaggi, L. Olcese, R. Biassoni, L. Moretta, P. Chavrier, A. Moretta, M. Daéron, E. Vivier, Reconstituted killer cell inhibitory receptors for major histocompatibility complex class I molecules control mast cell activation induced via immunoreceptor tyrosine-based activation motifs. *J. Biol. Chem.* **272**, 8989–8996 (1997).
47. T. Zech, C. S. Ejsing, K. Gaus, B. de Wet, A. Shevchenko, K. Simons, T. Harder, Accumulation of raft lipids in T-cell plasma membrane domains engaged in TCR signalling. *EMBO J.* **28**, 466–476 (2009).
48. B. F. Lillemeier, M. A. Mortelmaier, M. B. Forstner, J. B. Huppa, J. T. Groves, M. M. Davis, TCR and Lat are expressed on separate protein islands on T cell membranes and concatenate during activation. *Nat. Immunol.* **11**, 90–96 (2010).
49. S. Sasawatari, M. Yoshizaki, C. Taya, A. Tazawa, K. Furuyama-Tanaka, H. Yonekawa, T. Dohi, A. P. Makrigiannis, T. Sasazuki, K. Inaba, N. Toyama-Sorimachi, The Ly49Q receptor plays a crucial role in neutrophil polarization and migration by regulating raft trafficking. *Immunity* **32**, 200–213 (2010).
50. L. Olcese, P. Lang, F. Vély, A. Cambiaggi, D. Marguet, M. Bléry, K. L. Hippen, R. Biassoni, A. Moretta, L. Moretta, J. C. Cambier, E. Vivier, Human and mouse killer-cell inhibitory receptors recruit PTP1C and PTP1D protein tyrosine phosphatases. *J. Immunol.* **156**, 4531–4534 (1996).
51. N. T. Joncker, N. Shifrin, F. Delebecque, D. H. Raulet, Mature natural killer cells reset their responsiveness when exposed to an altered MHC environment. *J. Exp. Med.* **207**, 2065–2072 (2010).
52. J. M. Elliott, J. A. Wahle, W. M. Yokoyama, MHC class I-deficient natural killer cells acquire a licensed phenotype after transfer into an MHC class I-sufficient environment. *J. Exp. Med.* **207**, 2073–2079 (2010).
53. I. Poser, M. Sarov, J. R. Hutchins, J. K. Hériché, Y. Toyoda, A. Pozniakovsky, D. Weigl, A. Nitzsche, B. Hegemann, A. W. Bird, L. Pelletier, R. Kittler, S. Hua, R. Naumann, M. Augsburg, M. M. Sykora, H. Hofmeister, Y. Zhang, K. Nasmyth, K. P. White, S. Dietzel, K. Mechtler, R. Durbin, A. F. Stewart, J. M. Peters, F. Buchholz, A. A. Hyman, BAC TransgeneOmics: A high-throughput method for exploration of protein function in mammals. *Nat. Methods* **5**, 409–415 (2008).
54. L. Chiossone, J. Chaix, N. Fuseri, C. Roth, E. Vivier, T. Walzer, Maturation of mouse NK cells is a 4-stage developmental program. *Blood* **113**, 5488–5496 (2009).
55. **Acknowledgments:** We thank C. Beziers-Guigue (CIML) for excellent graphic assistance and CIML antibody and cytometry facilities. **Funding:** E.V. and S.U. are supported by grants from the Agence Nationale de la Recherche (ANR), Ligue Nationale contre le Cancer (Equipe labellisée “La Ligue”), and Fondation Del Duca. D.M. is supported by grants from the ANR, Institut National du Cancer, and Fondation pour la Recherche Médicale (Equipe labellisée FRM-2009). D.M., E.V., and S.U. are supported by institutional grants from INSERM, CNRS, and Université de la Méditerranée to the CIML. E.V. is a scholar of the Institut Universitaire de France. B.N.J. is supported by a fellowship from the Axa Research Fund. Y.M.K. is supported by a grant from Fondation pour la Recherche Médicale. **Author contributions:** S.G., B.N.J., S.P., S.M., T.T., A.F., N.C., T.W., and Y.M.K. performed and analyzed the experiments; S.G. and B.N.J. helped to prepare the manuscript; D.M. supervised and designed the FCS experiments; and E.V. and S.U. conceived and supervised the project, designed the experiments, and wrote the manuscript. **Competing interests:** E.V. is a cofounder and shareholder of Innate-Pharma.

Submitted 15 October 2010

Accepted 18 March 2011

Final Publication 5 April 2011

10.1126/scisignal.2001608

Citation: S. Guia, B. N. Jaeger, S. Piatek, S. Maifert, T. Trombik, A. Fenis, N. Chavrier, T. Walzer, Y. M. Kerdiles, D. Marguet, E. Vivier, S. Ugolini, Confinement of activating receptors at the plasma membrane controls natural killer cell tolerance. *Sci. Signal.* **4**, ra21 (2011).